We thank the reviewers for going through our manuscript titled "*Rapid formation of secondary aerosol precursors from the autoxidation of C_5–C_8 n-aldehydes*" and for their constructive suggestions on how to improve the work. We have incorporated all the suggestions and have modified the revised manuscript accordingly. Below, the reviewer queries are reproduced in red, followed by detailed point-by-point author responses in blue, and the changes and additions to the revised manuscript and the supplement in purple.

Referee #1

This paper reports the results of a thorough and carefully conducted experimental study of the formation of secondary aerosol precursors from the autooxidation of several long chain aldehydes. The topic is of current research interest to the atmospheric chemistry community. The results are presented clearly and concisely. The conclusions are well supported by the results. I recommend publication as is.

I noticed a couple of typos:

(1) On line 121, "we conducted the reactions at variable reaction times" might read better as "we studied the reactions over a range of reaction times".

Response: We thank the reviewer for the suggestion. Accordingly, changes are made in the revised manuscript.

Changes to manuscript: In line 133, "We studied the reactions over a range of reaction times (short: 1–3 s, and long: 11–13 s)."

(2) Calvert et al. "(2020)" should be "Calvert et al. (2011)" throughout.

Response: We thank the reviewer for pointing out this. The citation is now corrected as "Calvert et al. (2011)" throughout the text.

Referee #2

Review of "Rapid formation of secondary aerosol precursors from the autoxidation of C5-C8 n-aldehydes" by Barua, et al.

This paper reports on product observations of oxidation of suite of n-aldehydes in the presence of OH and other peroxy radicals with and without added NO. The study makes use of a nitrate (NO3-) chemical ionization mass spectrometer for product detection. The experiments are conducted in a flow tube-type of experiment at room temperature and 1 atmosphere, using the ozone reaction with tetra methyl ethylene as an OH source, analyzing products after a range of reaction times. Highly oxygenated molecules are observed to form after short reaction times (timescales of approx. 1-10 s) for all aldehydes studied, and the formation mechanism is proposed to occur through autoxidation reactions of peroxy radical intermediates.

General comments:

Generally, these results are very nice, following in step with a previous paper by the same first author. While this is a result demonstrating similar aldehydes behave like hexanal for longish RO2 lifetimes, I think the authors should add more value to this work, by extending this work beyond the previous paper. A simple kinetic model of the experiments would, substantially improve the understanding of the experiments, and allow more definitive statements to be made regarding the very important H-shift rate coefficients. Calibration and time-response/wall loss of the sensor and experiment apparatus needs to be discussed and may help authors report HOM yields. In addition, a simulation would lead to better understanding of the experiments with added NO.

Response: We thank the reviewer for the suggestion. We have now added a new section (*S13. Kinetic simulation*) in the Supplement. The section is reproduced at the end of the response to reviewer's final specific comment on Sect. 3.2 below (see pages 12–18).

We calibrated the instrument using sulfuric acid and determined the calibration coefficient of 2.0×10^9 molecule/cm^3/ncps and a detection limit of 2.82×10^3 molecules/cm^3 for sulfuric acid. The general quantification of HOMs (i.e., compounds with at least 6 O-atoms) in literature relies on the assumption that they are charged as efficiently as sulfuric acid. Thus, the same calibration coefficient was commonly used for estimating the concentrations of HOMs followed by their yields in this work.

The mass spectrometer that coupled to the flow reactor setup was very sensitive to changes in reactant gas flows. We observed an immediate response in the detected oxidation product intensities as shown in Figure S4 below. During the experiments, each reactant concentration was allowed to run for about 10–20 minutes.

Wall loss of reactive and condensable species is almost unavoidable phenomena in flow reactors and environmental chambers. Our experiments were performed in conventional flow reactors with wall interactions present. While discussing yield estimation, these influences are now discussed in Section S1 in the Supplement.

Addition to supplement: In lines 44–60, "We determined the calibration coefficient for our nitrate chemical ionization mass spectrometer (NO_3^--CIMS) to be 2.0×10^9 molecule/cm^3/ncps by calibrating the instrument for sulfuric acid using the method shown by Kürten et al. (2012). A detection limit (LOD) of 2.82×10^3 molecules/cm^3 for sulfuric acid was determined using the equation below.

$$LOD = \frac{3.3 \times \sigma}{S}$$

Here, S is the slope of the calibration curve and σ is the standard deviation of the responses of blank measurements. The HOMs were quantified based on the assumption that they are charged as efficiently as sulfuric acid. The concentrations of the oxidation products including HOMs were calculated by multiplying the individual normalized product signals with the calibration coefficient. The same calibration coefficient was commonly used for all oxidation products because of lack of methods that can account for differences in sensitivity across various

oxygenated products. Then, the yields of the products were estimated by dividing their concentrations with the concentration of consumed precursor VOC (i.e., Y_{HOM} = ΔHOM/ΔVOC). Also, note that the flow reactor system exhibits unavoidable wall loss of reactive and condensable species, which contributes to the overall uncertainty in the experimental yields. The normal uncertainty range with the measurement technique has been assumed as asymmetric -50% to +100% (about a factor of two)."

S5. Instrument's responses to changes in reactant flows

The mass spectrometer that used for detecting the oxidation products in different *n*-aldehyde experiments is very sensitive to the changes in reactant gas flow conditions. Figure S4 shows one minute average time series of several product signals that show responses of the detected signals increasing or decreasing depending on how the reactant gas flows are controlled. In Figure S4A, we can see that the reagent ion dimer $HNO_3NO_3^-$ drops immediately with the introduction of D_2O in the flow reactor and raises back with the withdrawal of the D_2O flow. The opposite trend is seen with the corresponding deuterated reagent dimer ion signal $DNO_3NO_3^-$. The product signal of $C_6H_{10}O_6$ gets exchanged with two D atoms and the corresponding $C_6H_8D_2O_6$ shows a similar trend as shown in the bottom part of Figure S4A. When the precursor VOC (hexanal) flow is set to zero, the signal of $C_6H_{10}O_6$ gets dropped completely. In Figure S4B, we can see how the octanal derived dominant $C_8H_{15}O_6$ radical signal responds with various NO flows. It shows a general decreasing trend with the increase of NO concentrations. On the other hand, the corresponding organonitrate $C_8H_{15}O_6NO$ signal raises with up to 200 ppb of NO and then drops with higher NO concentrations.

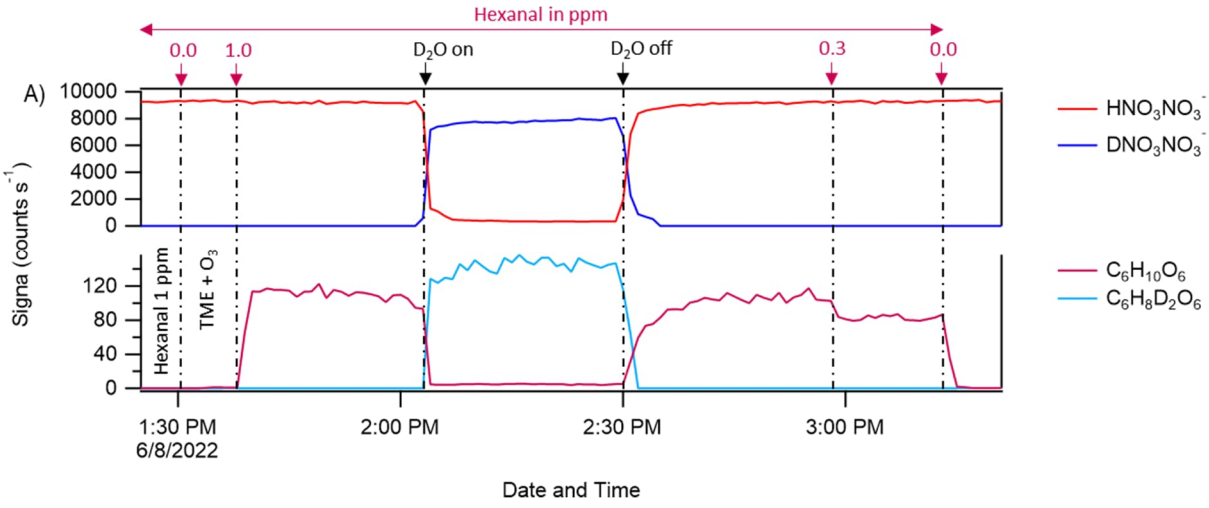

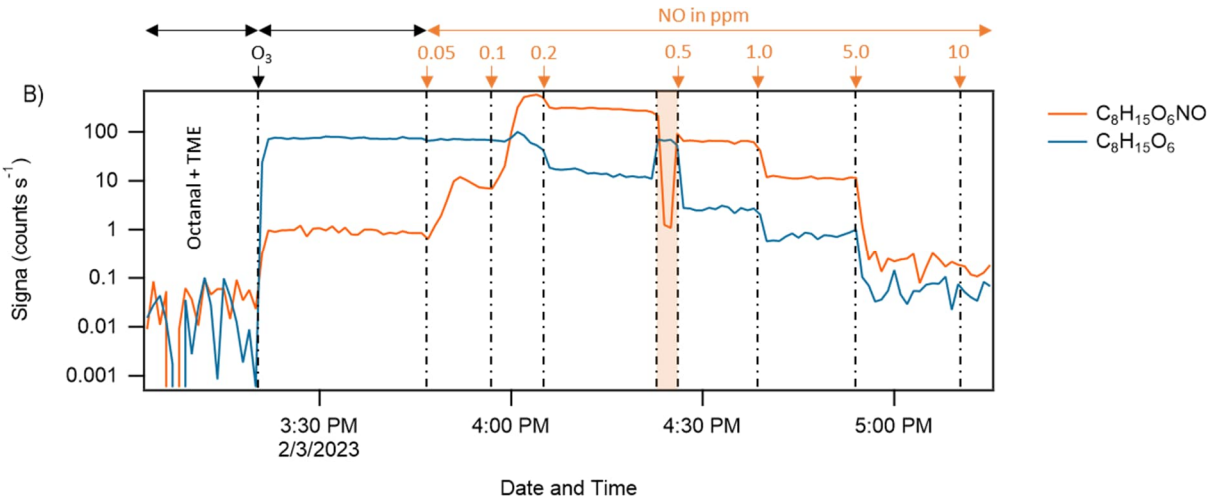

Figure S4. Time series of detected product signals with the changes in different reactant gas flows in OH initiated oxidation of hexanal (A) and octanal (B). The product signals are labelled with the exclusion of NO_3^- ion attachment in their compositions. Panel (A) shows that with the introduction of D_2O in the reaction mixture, labile H atoms in the reagent ion (top part) and in the oxidation product (bottom part) are exchanged with D atoms and the corresponding signals drop and raise accordingly. Panel (B) shows the responses of dominant $C_8H_{15}O_6$ radical and corresponding organonitrate $C_8H_{15}O_6NO$ with various NO flows. The shaded area in panel (B) indicates switching of NO mass flow controllers from smaller range to higher range.

Specific comments:

L82-83: 'autoxidation' needs to be more broadly defined… perhaps something like "Chain radical processes, generally starting with an oxygen-centered radical and leading to a carbon-centered radical species whose dominant fate is to add additional molecular oxygen." Most would consider alkoxy H-shifts and endocylization of peroxy and alkoxy radicals, with subsequent O2 addition to be examples of autoxidation.

Response: We thank the reviewer for pointing out this. Accordingly, we have now made changes to the definition of autoxidation in the revised manuscript.

Changes to manuscript: In lines 85–90, "Autoxidation refers to chain radical processes, generally starting with an oxygen-centered radical that undergoes unimolecular isomerization reaction leading to a carbon-centered radical species whose dominant fate is to add additional molecular oxygen and thus increases product O:C ratios (Crounse et al., 2013; Jokinen et al., 2014; Rissanen et al., 2014; Berndt et al., 2015; Mentel et al., 2015; Rissanen et al., 2015; Berndt et al., 2016)."

L91-96: Please also cite previous work on RO2 H-shifts from aldehydes. These have generally been found to be fast: https://doi.org/10.1021/jp108358y, https://doi.org/10.1021/jp211560u, https://doi.org/10.1021/acs.jpca.6b09370, https://doi.org/10.1021/acs.jpclett.9b01972, etc…

Response: We thank the reviewer for providing us with additional references. We have now added them as citations.

Addition to manuscript: In lines 97–99, "The fast aldehydic H-shift to the peroxy group is consistent with other carbonyl systems reported previously (Da Silva, 2011; Crounse et al., 2012; Møller et al., 2016, 2019)."

L101: replace 'besides' with 'In addition'?

Response: We thank the reviewer for the suggestion. Accordingly, changes are made in the revised manuscript.

Changes to manuscript: In lines 107–108, "In addition, the reactions were studied in the presence of variable concentrations of NO to examine ..."

L132: 'within' à 'below' ?

Response: In short reaction time experiments, 0.72 ppmv heptanal and 1 ppmv hexanal were used (listed in Table 1). We have now rephrased the sentence in question and replaced the ending "other aldehydes remained within 1 ppmv" by "other aldehydes were up to 1 ppmv".

Changes to manuscript: In lines 142–144, "In short reaction time experiments, the highest concentration of VOC (6.4 ppmv) was used for pentanal while the concentrations of other aldehydes were up to 1 ppmv."

L181-184(and other places): The term 'appeared' is unfortunately not quantitative. It would be more useful to the reader if some additional information were provided. This ties back to the general comments above regarding instrumental calibration/sensitivity, and noise level and response/wall-losses of the instrument. Ideally, something like XX fraction of 'aldehyde' molecules add 6 additional oxygen atoms within 2.1 s after reacting with OH, in absences of bimolecular reactions.

Response: We thank the reviewer for the suggestion. We have now replaced the word "appeared" by "formed" in line 212 and made changes from "appearance" to "observation" in other places in the revised manuscript. The reacted fraction of aldehyde is now mentioned as shown below. Moreover, while comparing the yields of oxidation products (in long residence time experiments) we now accounted for the precursor aldehyde consumption in each experiment and modified the y-axes in Figures 3 and 5 with % yields (see responses to latter comments).

Changes to manuscript: In lines 208–213, "As the reaction time increased, we observed the formation of monomeric HOM up to O_7 and accretion products up to O_{10} composition within 2.9 s in hexanal oxidation (see Fig. 2D) with the consumption of $\sim 8.88 \times 10^{-4}$ of its initial concentration. In the case of octanal, monomeric O_8 HOM and accretion products up to O_{10} formed within 2.1 s reaction time (see Fig. 2E) with a comparable reacted fraction ($\sim 8.71 \times 10^{-4}$) of its initial concentration."

Fig 1E: The bottom of this panel should be zoomed by ~4x on Y-axis.

Response: The bottom of Figure 2E (i.e., 1E in the previous version of the manuscript) is now zoomed by ~4x on y-axis (i.e., 0–35 × 10^{-6} ncps instead of previous 0–127 × 10^{-6} ncps) in the revised manuscript.

Changes to manuscript:

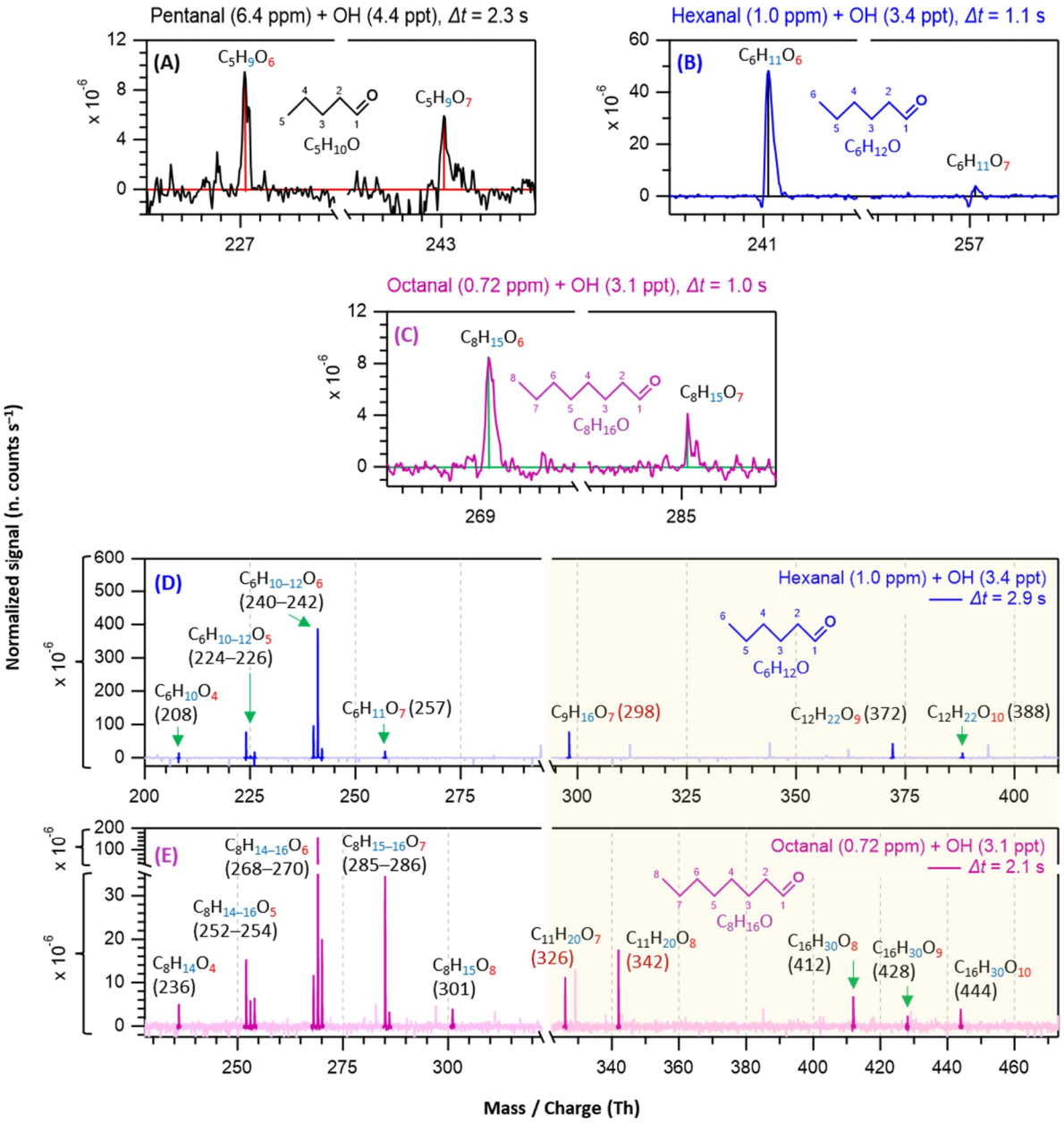

Figure 2. Nitrate chemical ionization mass spectra of OH initiated oxidation of *n*-aldehydes showing the formation of HOMs in different reaction times (Δt): 2.3 s – pentanal in black (A), 1.1 and 2.9 s – hexanal in blue (B and D), and 1.0 and 2.1 s – octanal in purple (C and E). The product peaks are labelled with the exclusion of NO_3^- ion attachment in their compositions. The backgrounds of TME ozonolysis (TME + O_3) and aldehyde have been subtracted from all spectra, resulting in several negative peaks in panels A–E. The accretion product region is highlighted in light gold background. The accretion products labeled with nominal mass/charge in dark red ($C_{n+3}H_{2n+4}O_{7–8}$) are related to the TME-derived peroxy radical $C_3H_5O_3$.

Figs 1,2,6: There are negative going peaks in these figures, which leads to the question of what is being shown in the figures. Please explain the data processing in the text, ie is some background being subtracted off? This can also lead into a discussion of response times (when zeroing or starting/stopping expt).

Response: We thank the reviewer for pointing out this. The backgrounds of TME ozonolysis (TME + O_3) and aldehyde were subtracted from the spectra for clarity. We have now mentioned this in the captions of Figures 2, 3, and 7 (i.e., previous Figs. 1, 2, and 6) in the revised manuscript. We have now added a new section (*S4. TME ozonolysis and aldehyde background spectra*) in the Supplement showing some persistent background signals (see below).

Discussion about the instrument's responses to changes in experimental conditions are now added in Section S5 in the Supplement. The section is reproduced at the end of the response to reviewer's general comments above (see pages 3–4).

Changes to manuscript: In Figure 2 caption lines 219–220, "The backgrounds of TME ozonolysis (TME + O_3) and aldehyde have been subtracted from all spectra, resulting in several negative peaks in panels A–E."

In Figure 3 caption lines 245–246, "The backgrounds of TME ozonolysis (TME + O_3) and aldehyde have been subtracted from all spectra, resulting in several negative peaks in panels A–D."

In Figure 7 caption lines 339–341, "The backgrounds of TME ozonolysis (TME + O_3) and aldehyde have been subtracted from the spectra, resulting in several negative peaks in panels A–B."

Addition to supplement:

S4. TME ozonolysis and aldehyde background spectra

To ensure that the *n*-aldehyde + OH oxidation products shown in Figures 2, 3, 5, and 7 of the main manuscript are either distinct or significantly bigger than any background signals, we record all the possible background spectra separately. Figure S3 clearly shows that there are some persistent background signals with nominal mass/charge 226 (panels b–c), 276 (panels b–c), 283 (panel a), 292 (panels a–d), 412 (panels c–d), 440 (panels a and d), etc. present. While most of them are distinct from the nominal mass/charge ratios of the products signals in *n*-aldehyde oxidation, a few of them match with the oxidation products (e.g., m/z 226 with $C_5H_8O_6$ and $C_6H_{12}O_5$, m/z 342 with $C_{11}H_{20}O_8$, and m/z 412 with $C_{16}H_{30}O_8$). Therefore, the backgrounds of TME ozonolysis (TME + O_3) and relevant aldehyde are subtracted from the spectra reported in the main manuscript (Figures 2, 3, and 7) for clarity and thus it ensures that the reported product signals are produced exclusively during the oxidation of *n*-aldehydes.

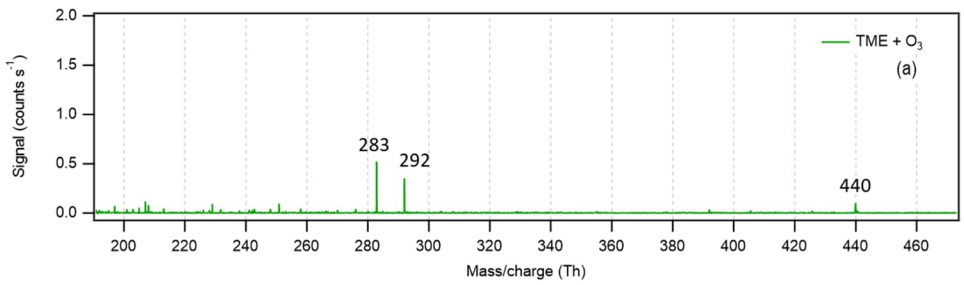

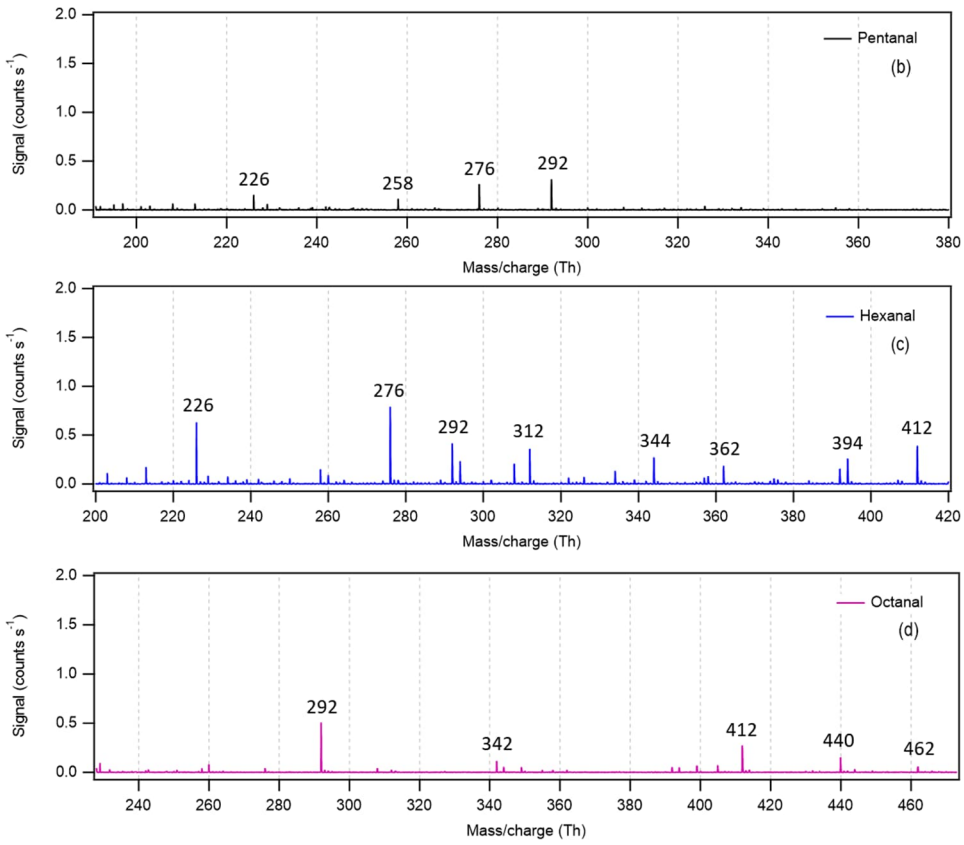

Figure S3: Individual background spectra of TME + O_3 (a), pentanal (b), hexanal (c), and octanal (d) recorded during *n*-aldehyde OH oxidation experiments. The reaction of TME + O_3 is the source of the oxidant OH.

General comment: As a reader, I want know more about how your experiment evolves as a function of time. A simple kinetic simulation would quickly allow the authors to plot time profiles of the various reactants and products in the system, and would help readers to better understand the experiment.

Response: We thank the reviewer for the suggestion. We have now added a new section (*S13. Kinetic simulation*) in the Supplement including the time profiles of precursor aldehydes, NO, O_3, OH and initial RO_2 radicals under different experimental conditions. The section is reproduced at the end of the response to reviewer's final specific comment on Sect. 3.2 below (see pages 12–18).

L219-220: To jump from comparing signals (shown in figure) to comparing yields (in text) one must be making some assumption about sensitivities… explicitly state what is being assumed for sensitivity in text.

Response: We thank the reviewer for pointing out this. In the revised manuscript in Figure 4, we have now modified the numbers in y-axis by percentage yields (measured oxidation product concentrations divided by consumed VOC). Also, assumption about sensitivities is included in Section S1 in the Supplement.

Changes to manuscript:

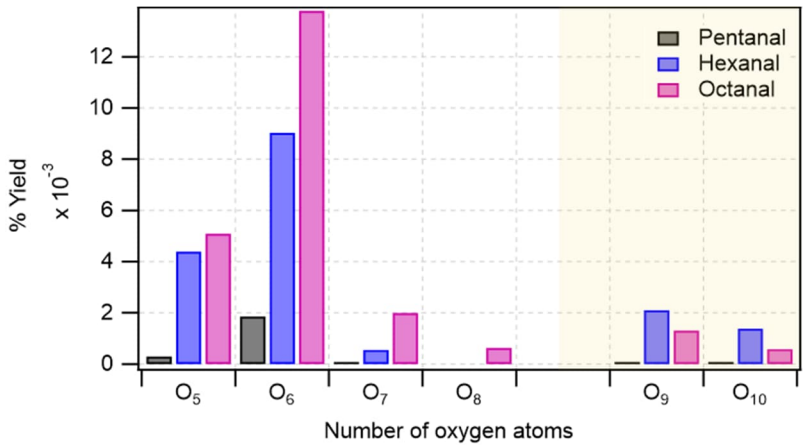

Figure 4. Distribution of major oxidation products (O_5–O_8 in monomeric regime with white background, and O_9–O_{10} in accretion product regime with light gold background) in pentanal, hexanal, and octanal oxidation initiated by OH radical. In y-axis, the numbers are the cumulative sum of yields of products with the same oxygen number. Reaction time, Δt = 11–13 s.

Addition to supplement: In lines 44–57, "We determined the calibration coefficient for our nitrate chemical ionization mass spectrometer (NO_3^--CIMS) to be 2.0×10^9 molecule/cm^3/ncps by calibrating the instrument for sulfuric acid using the method shown by Kürten et al. (2012). A detection limit (LOD) of 2.82×10^3 molecules/cm^3 for sulfuric acid was determined using the equation below.

$$LOD = \frac{3.3 \times \sigma}{S}$$

Here, S is the slope of the calibration curve and σ is the standard deviation of the responses of blank measurements. The HOMs were quantified based on the assumption that they are charged as efficiently as sulfuric acid. The concentrations of the oxidation products including HOMs were calculated by multiplying the individual normalized product signals with the calibration coefficient. The same calibration coefficient was commonly used for all oxidation products because of lack of methods that can account for differences in sensitivity across various oxygenated products. Then, the yields of the products were estimated by dividing their concentrations with the concentration of consumed precursor VOC (i.e., Y_{HOM} = ΔHOM/ΔVOC)."

L222-227: This could be diagnosed with kinetic simulation.

Response: We thank the reviewer for the suggestion and diagnosed this (i.e., difference in dimer to monomer ratios between hexanal and octanal oxidation experiments) using kinetic simulation. Indeed, simulation results show that both precursors produced comparable quantities of initial RO_2 radicals (9.12×10^9 and 9.37×10^9 molecules cm^{-3} from octanal and hexanal, respectively).

Changes to manuscript: In lines 252–259, "In the accretion product regime, the yields of O_9–O_{10} products in octanal are lower than that of hexanal which is also reflected in their dimer to monomer ratios with octanal being 8.8×10^{-2} and hexanal being 2.5×10^{-1}. The lower ratio for octanal compared to hexanal is observed despite both precursors producing comparable quantities of initial RO_2 radicals (9.12×10^9 and 9.37×10^9 molecules cm^{-3} from octanal and hexanal, respectively; see Table S1 in the Supplement). This can lie in the variation of RO_2 + RO_2 reaction rate coefficients forming the accretion products ($RO_2 + RO_2 \rightarrow ROOR + O_2$) which is highly dependent on specific RO_2 structures (Berndt et al., 2018; Shallcross et al., 2005)."

L236-237: This could be phased more clearly.

Response: We thank the reviewer for the suggestion. The sentence in question is now rephrased and split into two for clarity.

Changes to manuscript: In lines 267–271, "It has been widely acknowledged that the formation of HOM is suppressed in high NO_x conditions (Wildt et al., 2014; Praske et al., 2018; McFiggans et al., 2019; Pullinen et al., 2020), thus reducing the SOA yields. In this process, the reduction in SOA yield is largely attributed to the suppression of highly condensable HOM accretion products ($RO_2 + RO_2 \rightarrow ROOR$) (Kirkby et al., 2016; Pullinen et al., 2020)."

Sect 3.2: What do the profiles of NO and O3 look like across these experiments? The lifetime of NO with 200 ppbv O3 is ~0.02s. Similarly, the lifetime of O3 with 1 ppmv NO is ~0.005s. This will almost certainly impact the interpretation of the results as when NO < O3 most of the NO will react with O3, and 'average' NO seen by peroxy radicals will be much less than initial NO. When NO>O3, O3 is largely titrated by NO, making much less OH available to react with the aldehyde. When NO and O3 are very similar one may actually maximize total OH production due to recycling of OH from HO2 + OH. To increase the usefulness of Fig 5, the points need to be normalized by total aldehyde reacting with OH across experiment, and x-axis labeled with 'average' NO rather than initial NO (perhaps weighted by [OH] profile). A kinetic simulation of the experiments will help enable this.

There was an error estimating the lifetimes of O3 and NO in the original comment of referee 2. The final paragraph should read:

Sect 3.2: What do the profiles of NO and O3 look like across these experiments? The lifetime of NO with 200 ppbv O3 is ~10s. Similarly, the lifetime of O3 with 1 ppmv NO is ~2s. This will impact the interpretation of the results as reactants will significantly change over the course of the experiment. When NO>>O3, O3 will significantly react with NO, making less OH available to react with the aldehyde. When NO and O3 are very similar one may actually maximize total OH production due to recycling of OH from HO2 + OH. To increase the usefulness of Fig 5, the points need to be normalized by total aldehyde reacting with OH across experiment, and x-axis labeled with 'average' NO rather than initial NO (perhaps weighted by [OH] profile). A kinetic simulation of the experiments will help enable this.

Response: We thank the reviewer for this insightful comment and agree with the thoughts around atmospheric lifetimes (τ) of NO and O_3 with respect to each other and concerns about how their initial concentrations can affect the oxidant OH radical concentration. We have now added a new section (*S13. Kinetic simulation*) in the Supplement describing the estimated OH and initial RO_2 radicals under various initial NO conditions. The reaction, HO_2 + NO that recycles OH radicals is included in the simulation. Note that even at 1 ppmv initial NO condition, atmospherically relevant concentrations of average OH radicals (2.6–3.1 × 10^6 molecules cm^{-3}) are estimated (Table S1 below). The time profiles of NO and O_3 under different experimental conditions are presented in Figure S17 in the Supplement (see below).

In the revised manuscript, we also modified Figure 6 by providing percentage yields instead of normalized signal intensities (taking account the concentrations of reacted precursor aldehyde, i.e., *Δ*VOC) in the y-axis and average NO instead of initial NO in the x-axis. In addition, the average concentration of OH radicals corresponding to each NO condition is displayed in Figure 6.

Changes to manuscript:

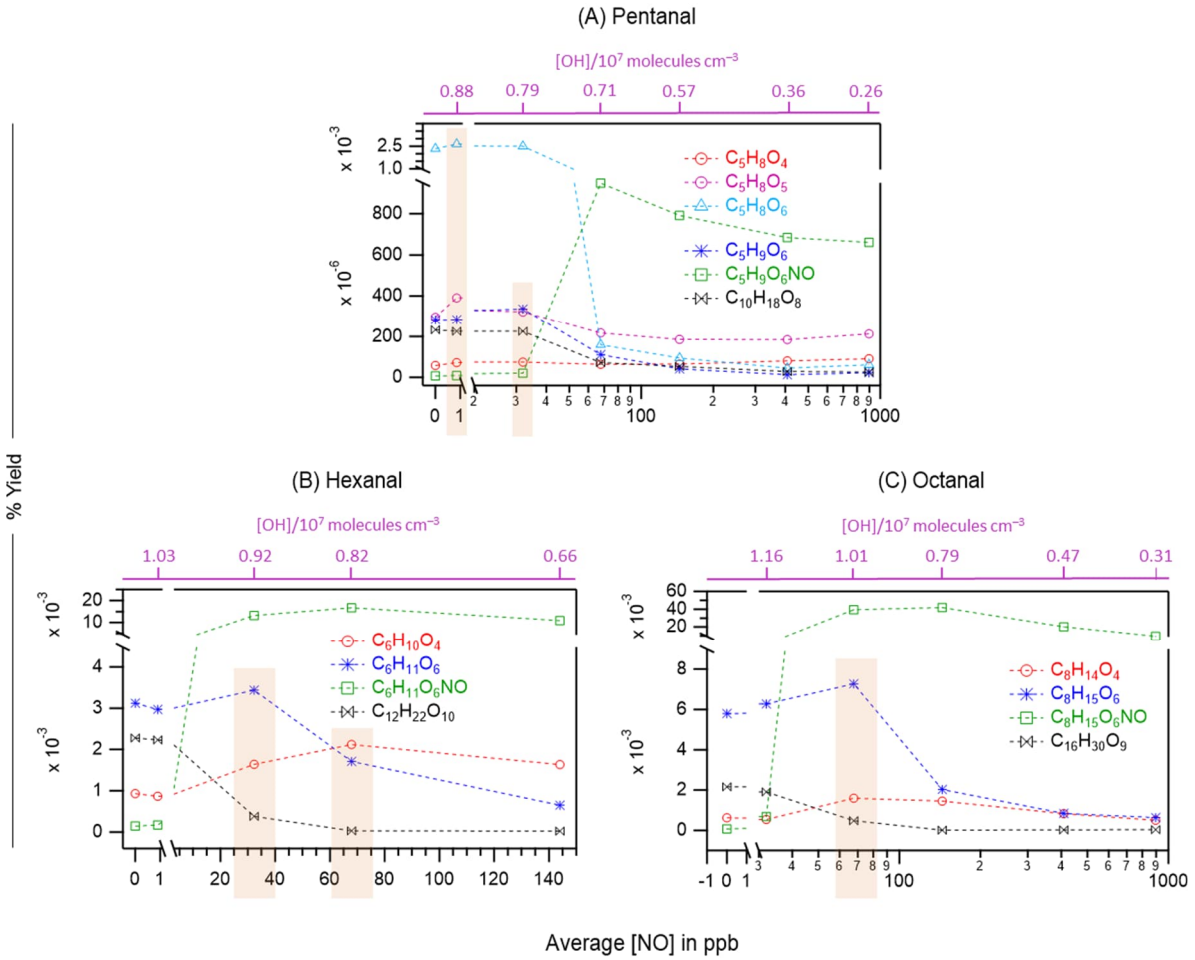

Figure 6. The yields of different oxidation products including monomeric HOMs, organonitrates (green markers), and HOM accretion products (black markers) as a function of average NO concentrations in OH initiated oxidation of n-aldehydes: pentanal (A), hexanal (B), and octanal (C). The corresponding average OH radical concentrations in these

experiments are shown with purple scales. Note the logarithmic scale (x-axis) in panels A and C. The orange rectangles highlight the enhanced yields of several non-nitrogen containing products: O_4–O_6 closed-shell products from pentanal under around 1 ppb NO (A), O_4 closed-shell products from hexanal and octanal under around 70 ppb NO (B and C), O_6 peroxy radical from pentanal and hexanal under around 30 ppb NO (A and B) and the same from octanal under 70 ppb NO (C). Reaction time, Δt = 11–13 s.

Addition to manuscript:

2.2 Kinetic simulation

We estimated the concentrations of reactive species in the flow reactor during different *n*-aldehyde oxidation experiments using a kinetic simulator Kinetiscope (version 1.1.1136.x64) (Hinsberg and Houle, 2022). These include the average concentrations of OH radicals and initial RO_2 radicals (i.e., $C_nH_{2n-1}O_3$, the first peroxy radicals formed in the oxidation process) produced in the experiments. In the simulations, a single-reactor model with constant volume, pressure, and temperature was employed. The temperature was set to 298.15 K. The simulation setting parameters such as total number of particles (1×10^9) and random number seed (12947) were kept constant for consistency, while the maximum simulation time was matched to that of individual experiments. Details of all the simulations are provided in Sect. S13 in the Supplement.

Addition to supplement:

S13. Kinetic simulation

S13.1 Simulations without and with NO

Chemical kinetic simulations were carried out using Kinetiscope Program (Bunker et al., 1974; Gillespie, 1976; Hinsberg and Houle, 2022) to estimate the concentrations of oxidant OH and initial RO_2 radicals in different *n*-aldehyde oxidation reactions without (reaction steps 1–3, 8–10 below) and with the presence of NO (reaction steps 1–12 below). For the reactions of different *n*-aldehydes with OH radical, we used the rate coefficients of 2.66×10^{-11}, 2.85×10^{-11}, and 3.0×10^{-11} cm^3 molecule^{-1} s^{-1} for pentanal (PTL), hexanal (HXL), and octanal (OTL), respectively, reported by Mellouki et al. (2015). In our flow reactor setup, we produced OH radicals in situ by the ozonolysis reaction of tetramethyl ethylene (TME). The produced OH radicals react with TME as well as with the aldehyde in the flow reactor. In the simulations, we used reaction rate coefficients k_{TME-O_3} of 1.5×10^{-15} and k_{TME-OH} of 1.0×10^{-10} cm^3 molecule^{-1} s^{-1} accounting for the reactions of TME with ozone and OH, respectively (Manion et al., 2015). The initial precursor concentrations of aldehyde, TME, ozone, and NO identical to the experimental conditions (see Table S1 below) were used. These include 1.3–2.5 ppm ($6.15–3.20 \times 10^{13}$ molecules cm^{-3}) of pentanal, 1 ppm (2.46×10^{13} molecules cm^{-3}) of hexanal, 0.72 ppm (1.77×10^{13} molecules cm^{-3}) of octanal, 43.2–48.2 ppb ($1.06–1.19 \times 10^{12}$ molecules cm^{-3}) of TME, and 208–295 ppb ($5.12–7.26 \times 10^{12}$ molecules cm^{-3}) of ozone. In the flow reactor experiments, high VOC concentrations were used to scavenge OH, especially as TME reacts so fast with it. Following the reaction of aldehyde with OH, the initially formed carbon centered radical readily undergoes a pseudo unimolecular

reaction with O_2 to form the first RO_2 radical. For simplification, we show the formation of different RO_2 radicals directly from the reactions of aldehyde with OH, and TME with OH. Here, TME-produced RO_2 and aldehyde-produced RO_2 are separated by the expressions RO_2_T and RO_2_A, respectively.

With the addition of NO in the reaction system, it is expected to influence the concentrations of OH radicals and initial RO_2 radicals. Therefore, to simulate the experiments with NO, we included the bimolecular reaction rate coefficients of $k_{NO-OH} = 3.3 \times 10^{-11}$, $k_{HONO-OH} = 6.0 \times 10^{-12}$, $k_{NO-O_3} = 1.8 \times 10^{-14}$, and $k_{NO_2-OH} = 4.1 \times 10^{-11}$ cm^3 $molecule^{-1}$ s^{-1} (Atkinson et al., 2004), with respect to their corresponding reactions in the simulation. In addition, bimolecular rate coefficients for RO_2 + RO_2 and RO_2 + NO reactions were set to the generic values of 3.2×10^{-11} and 9.0×10^{-12} cm^3 $molecule^{-1}$ s^{-1}, respectively (Berndt et al., 2018; Jenkin et al., 2019) to account for sinks of RO_2 radicals. The influences of NO + HO_2, RO_2 + HO_2, and RO_2 + NO_2 reactions on OH and RO_2_A radical concentrations were examined separately and discussed in the section below. An example of the reaction steps used in the current simulation is as follows. The results are shown in Figure S16 and Table S1.

1. TME + O_3 => OH ($k_{TME-O_3} = 1.5 \times 10^{-15}$ cm^3 $molecule^{-1}$ s^{-1})
2. TME + OH => RO_2_T ($k_{TME-OH} = 1.0 \times 10^{-10}$ cm^3 $molecule^{-1}$ s^{-1})
3. OTL + OH => RO_2_A ($k_{OTL-OH} = 3.0 \times 10^{-11}$ cm^3 $molecule^{-1}$ s^{-1})
4. NO + OH => HONO ($k_{NO-OH} = 3.3 \times 10^{-11}$ cm^3 $molecule^{-1}$ s^{-1})
5. HONO + OH => H_2O + NO_2 ($k_{HONO-OH} = 6.0 \times 10^{-12}$ cm^3 $molecule^{-1}$ s^{-1})
6. NO + O_3 => NO_2 + O_2 ($k_{NO-O_3} = 1.8 \times 10^{-14}$ cm^3 $molecule^{-1}$ s^{-1})
7. NO_2 + OH => HNO_3 ($k_{NO_2-OH} = 4.1 \times 10^{-11}$ cm^3 $molecule^{-1}$ s^{-1})
8. 2 RO_2_T => Sink_a ($k_{RO_2-RO_2} = 3.2 \times 10^{-11}$ cm^3 $molecule^{-1}$ s^{-1})
9. 2 RO_2_A => Sink_b ($k_{RO_2-RO_2} = 3.2 \times 10^{-11}$ cm^3 $molecule^{-1}$ s^{-1})
10. RO_2_T + RO_2_A => Sink_ab ($k_{RO_2-RO_2} = 3.2 \times 10^{-11}$ cm^3 $molecule^{-1}$ s^{-1})
11. RO_2_T + NO => $RONO_2$ ($k_{RO_2-NO} = 9.0 \times 10^{-12}$ cm^3 $molecule^{-1}$ s^{-1})
12. RO_2_A + NO => $RONO_2$ ($k_{RO_2-NO} = 9.0 \times 10^{-12}$ cm^3 $molecule^{-1}$ s^{-1})

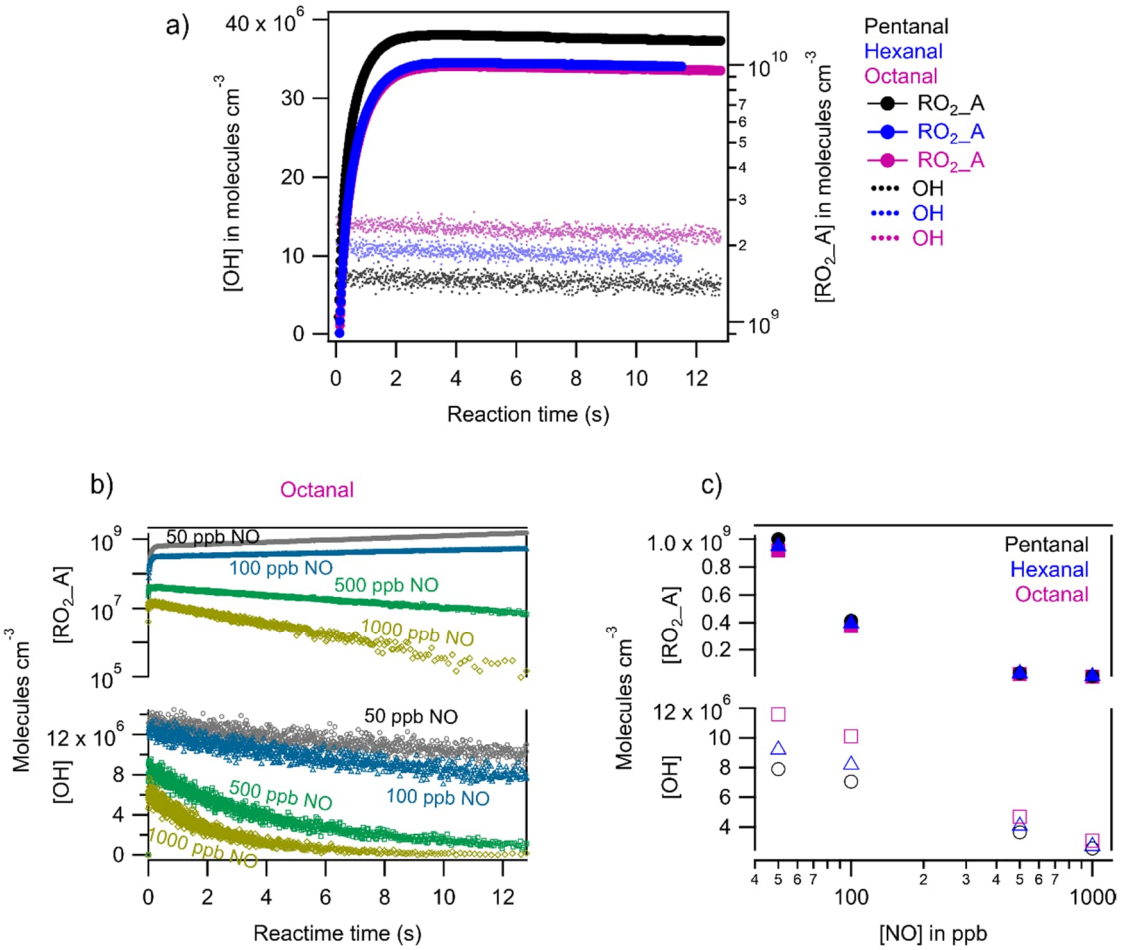

Figure S16. Concentration profiles of OH and initial RO_2_A radicals produced in *n*-aldehyde oxidation derived by chemical kinetic simulations under laboratory flow reactor experimental condition without NO (a) and with NO (b–c). Panel (b) shows results from octanal. In panel (c), average concentrations of OH and RO_2_A radicals during 11–13 s reaction time are presented in open and filled markers, respectively.

Figure S16a and Table S1 imply that the average concentrations of oxidant OH and initial RO_2_A radicals in the flow reactor are comparable in different *n*-aldehyde oxidation experiments. In the experiments without NO, the simulation produced average concentrations of OH radicals are 6.78×10^6, 1.03×10^7, and 1.33×10^7 molecules cm^{-3} for the experiments with PTL, HXL, and OTL, respectively.

Table S1. Average concentrations of OH and initial RO_2 radicals and reacted precursor aldehyde concentrations (ΔVOC) in different *n*-aldehyde oxidation experiments derived from kinetic simulations under laboratory conditions. Reaction time, Δt = 11–13 s.

Expt. type (VOC)	Model input				Model output		
	[VOC] ppmv	[TME] ppbv	[O_3] ppbv	[$NO]_{t=0}$ ppbv	Δ[VOC] ppbv	[OH] #/cm^3	[RO_2_A] #/cm^3
Simulation without NO							
PTL	2.5	48.2	295	–	5.78	6.78×10^6	1.21×10^{10}
HXL	1.0	43.2	225	–	3.39	1.03×10^7	9.37×10^9
OTL	0.72	48.2	208	–	3.65	1.33×10^7	9.12×10^9
In the presence of NO							
PTL	1.3	48.2	208	0	3.91	8.84×10^6	9.67×10^9
				50	3.42	7.90×10^6	1.00×10^9
				100	2.98	7.06×10^6	4.14×10^8
				500	1.09	3.64×10^6	3.26×10^7
				1000	0.43	2.55×10^6	1.05×10^7
HXL	1.0	43.2	225	50	2.96	9.22×10^6	9.49×10^8
				100	2.58	8.20×10^6	3.96×10^8
				500	0.98	4.09×10^6	3.06×10^7
				1000	0.38	2.72×10^6	9.34×10^6
OTL	0.72	48.2	208	50	3.12	1.16×10^7	9.18×10^8
				100	2.67	1.01×10^7	3.71×10^8
				500	0.88	4.70×10^6	2.64×10^7
				1000	0.33	3.09×10^6	7.98×10^6

The corresponding estimated RO_2_A radical concentrations are 1.21×10^{10}, 9.37×10^9, and 9.12×10^9 molecules cm^{-3}, respectively. While the average OH concentrations for HXL and OTL experiments are closer to each other, it is somewhat lower for the PTL experiment by a factor of 1.5 to 2 despite having higher initial ozone concentration. This can be attributed to the OH radical consumption by higher precursor PTL concentration compared to that of HXL and OTL. It is reflected in the concentrations of initial RO_2_A radicals in the three studied systems which are rather comparable and we aim for this as the starting condition for autoxidation. Note the sequential increase in reaction rate coefficients of aldehydes (from PTL to OTL) with OH radical mentioned above. In the presence of NO, Figure S16b shows how the concentration profiles of OH and RO_2_A radicals evolve in time with OTL oxidation experiment as an example. In all the *n*-aldehyde systems studied, the primary RO_2_A radical concentration steadily increases with time under 50 ppb and 100 ppb initial NO conditions. However, at 500 ppb and 1000 ppb NO conditions, the concentrations of RO_2_A radicals decrease with time soon after achieving their initial peak values. In the case of OH radicals, the concentrations show a general decreasing trend with time while at higher NO conditions (from 500 ppb initial NO), we observe a faster decreasing tendency in concentrations as expected. It is also rewarding to see that the initial RO_2_A radical concentrations from the studied *n*-aldehydes are comparable under various NO conditions (see Figure S16c and Table S1). Furthermore, it is important to mention that the concentrations of oxidant OH and primary

RO_2_A radicals reported here are at their upper limits as the loss of the radicals to the reactor wall is not accounted. Therefore, in our flow reactor experiments, the concentrations of the reactive radical species are close to the expected concentrations in the ambient air, and we believe they are well representative.

Under higher initial NO conditions, OH radical concentrations are depleted predominantly via its reaction with NO (reaction step 4) as well as via the drop of reactant ozone (reaction step 6) concentrations. Figure S17 shows the time series of NO, O_3, and precursor aldehyde concentrations estimated by the simulations. A faster drop of ozone concentrations is seen under higher initial NO concentrations of 500 ppb and above compared to lower NO concentrations (panels a, c and e of Figure S17). This is reflected in the estimated OH concentrations (Figure S16c and Table S1) as well as in the consumption of precursor aldehydes (see panels b, d and f of Figure S17, and ΔVOC in Table S1).

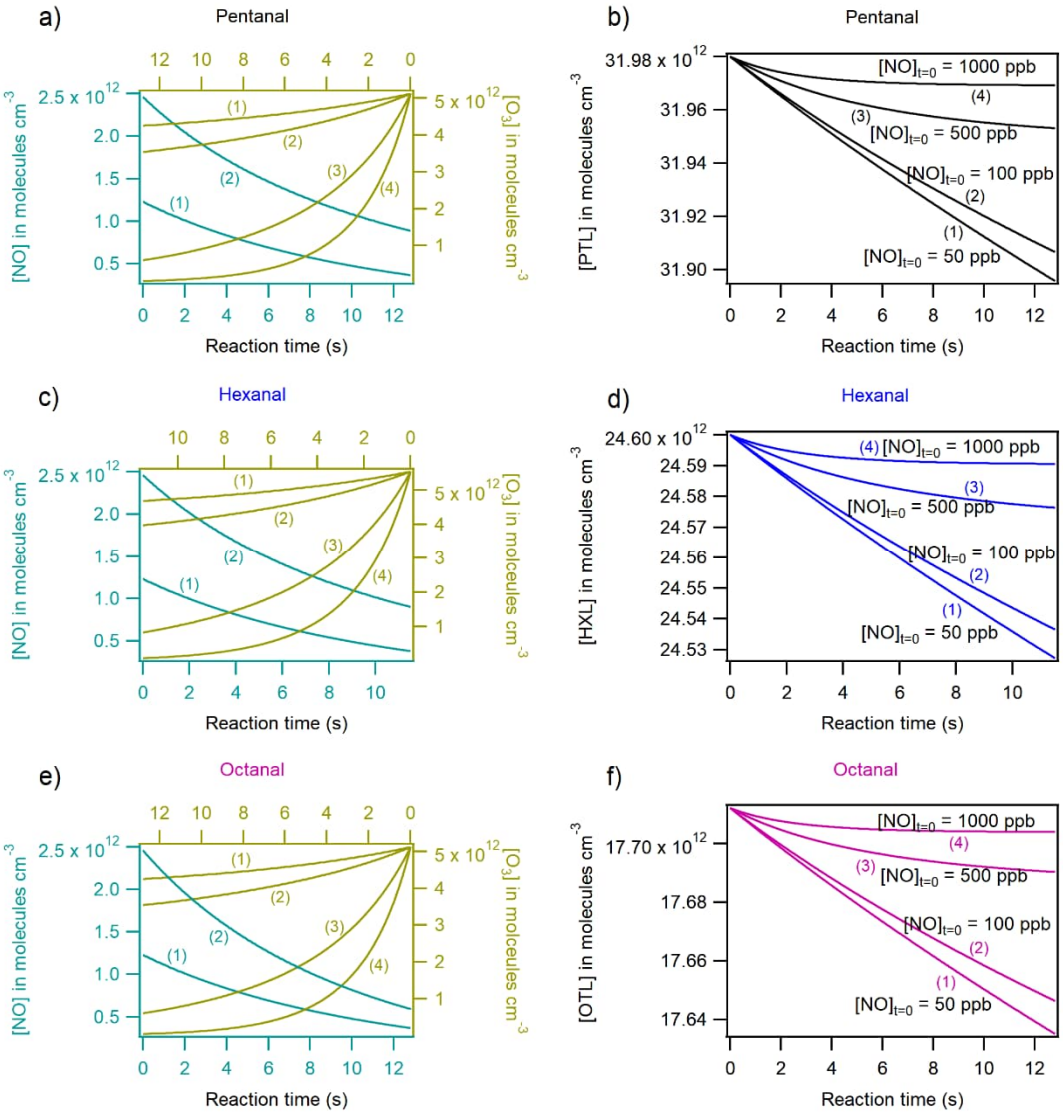

Figure S17. Concentration profiles of NO, O_3, and *n*-aldehyde as a function of reaction time under different initial $[NO]_{t=0}$ conditions: pentanal (a–b), hexanal (c–d), and octanal (e–f). The initial NO conditions are marked with numbers within parenthesis: $[NO]_{t=0}$ = 50 ppb (1),

$[NO]_{t=0}$ = 100 ppb (2), $[NO]_{t=0}$ = 500 ppb (3), and $[NO]_{t=0}$ = 1000 ppb (4). Reaction time, Δt = 11–13 s. PTL = pentanal, HXL = hexanal, and OTL = octanal.

S13.2 Impact of HO_2 on OH and RO_2

In the gas-phase oxidation process of volatile organic compounds (VOCs), it is usual to produce hydroperoxy radicals (HO_2) alongside the production of alkyl peroxy radicals (RO_2). In the presence of NO, the HO_2 radicals react with NO to recycle OH and NO_2 radicals in the reaction system (see reaction step 13) (Atkinson et al., 2004). In addition, the reaction of HO_2 with RO_2 can produce closed shell hydroperoxide (ROOH) along with other products (Boyd et al., 2003). Here, we included these reactions as other sinks of RO_2 in the simulation (reaction steps 14–15).

13. HO_2 + NO => OH + NO_2 (k_{HO_2-NO} = 8.91 × 10^{-12} cm^3 $molecule^{-1}$ s^{-1})
14. RO_2_T + HO_2 => Sink_c ($k_{RO_2-HO_2}$ = 2.2 × 10^{-11} cm^3 $molecule^{-1}$ s^{-1})
15. RO_2_A + HO_2 => Sink_d ($k_{RO_2-HO_2}$ = 2.2 × 10^{-11} cm^3 $molecule^{-1}$ s^{-1})

In the flow reactor system, we presume that the production of HO_2 radicals is about 30% of total RO_2 radicals (RO_2_T + RO_2_A) during the reaction time. Therefore, to examine the influence of the HO_2 reactions with NO and RO_2 on the concentrations of OH and RO_2_A radicals, we ran a separate set of simulations on Kinetiscope including the reaction steps 13–15. An initial HO_2 concentration of 30% of total RO_2 (e.g., 1.35 × 10^8 molecules cm^{-3} of HO_2 in OTL oxidation at 100 ppb initial NO condition) obtained from the previous simulation without HO_2 was used in the subsequent simulation. Figure S18 shows the results of HXL and OTL oxidation processes without and with involving the reaction steps 13–15. In all *n*-aldehyde simulations, the reaction steps 13–15 do not seem to alter the average concentrations of OH and RO_2_A radicals given that the reaction scheme (reaction steps 1–15) is lacking a constant source of 30% HO_2. To examine the maximum possible OH recycling from the reaction step 13, we also conducted another set of simulations by excluding reaction steps 14–15. Again, this approach reproduced the same levels of average OH and RO_2_A concentrations highlighting that the OH radical recycling under the studied NO conditions are not likely significant.

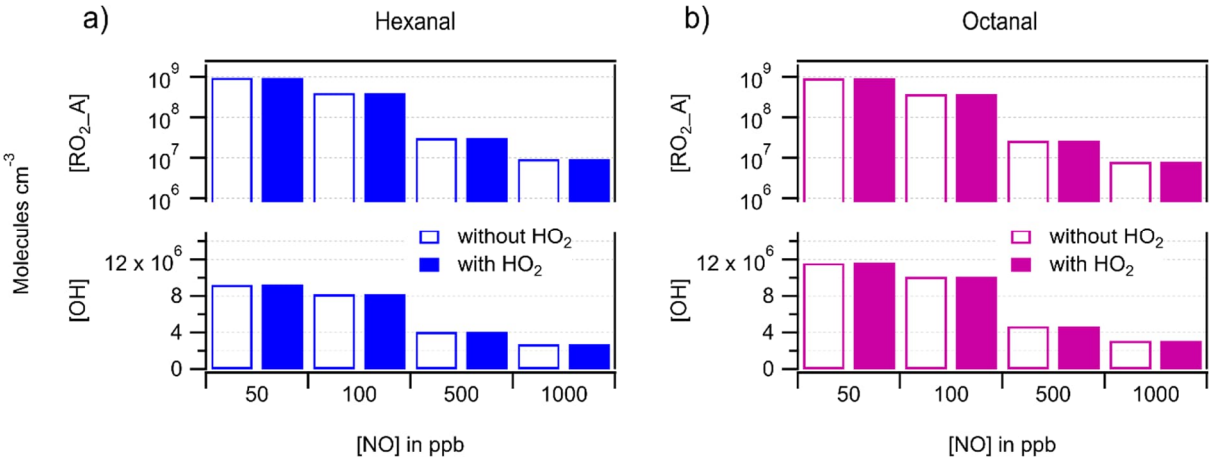

Figure S18. Average concentrations of OH and initial RO_2_A radicals produced in hexanal (a) and octanal (b) oxidation derived by chemical kinetic simulations under laboratory conditions with varying initial NO. Simulations that include the reactions of HO_2 with NO and RO_2 (reaction steps 13–15) are presented in filled bars while simulations without these reaction steps are presented in open bars.

Referee #3

Barua et al report HOMs formation of C5-C8 linear aldehydes and effect of chain length on autoxidation of C5-C8 aldehyde. HOMs were formed in a flow tube and detected by using NO3--CIMS. The authors found that octanal reached same level oxygenation (form O7-HOM)in shorter time than pentanal. At similar reaction time (11-13s), increasing oxygenation and higher intensity of HOMs signal were observed for C5-C8 aldehydes. HOMs formation mechanism of pentanal is applicable to C5-C8 aldehydes, shown by D2O experiments. NO suppressed accretion products but enhanced some of the monomeric HOMs. Some HOMs (O4-O6) were not suppressed by NO up to 50-100 ppb NO.

Aldehyde is a class of important atmospheric VOCs. Their oxidation may contribute largely to formation of low-volatility organics and thus to secondary organic aerosol. Therefore, understanding the HOMs formation of aldehydes have critical atmospheric significance. The experiments in this study are well designed. The manuscript is generally well-written. I have the follows comments for the authors to consider.

Specific comments

1. The comparison of various aldehydes on "the reactivity and HOM formation potential" is mostly based on whether HOMs can be observed at certain times, or precursor concentrations required, and/or signal intensity (e.g. L16-19, L166-167). Such a comparison is somewhat not systematic, in my opinion. Is there a way to provide the HOM yield or kinetic parameters and make direct comparison of different aldehydes?

Response: We thank the reviewer for the comment. The formation of HOMs in short reaction time experiments depends on how fast the first alkyl peroxy radicals (RO_2) form as well as how fast the subsequent isomerization reactions are. For example, within 1–2 s rection time, pentanal did not produce any HOMs regardless of how high the precursor concentrations were.

We have now conducted kinetic simulations using experimental conditions. The simulation results show that the reacted concentrations (ΔVOC) of pentanal, hexanal, and octanal were 1.15, 0.34, and 0.30 ppb, respectively, in their short reaction time experiments of 2.3, 1.1, and 1.0 s, respectively, to form the observed HOMs. Unfortunately, we could not measure the VOC consumption. We have also provided the percentage yields instead of normalized signal intensities of the reaction products in Figures 4 and 6 in the revised manuscript.

Changes to manuscript: In lines 191–194, "... with the increase of number of carbon atoms in the studied aldehydes, the required precursor concentrations for first HOM observation decreased (from 6.4 ppm pentanal, 1 ppm hexanal to 0.72 ppm octanal; corresponding reacted concentrations 1.15, 0.34, and 0.30 ppb, respectively)."

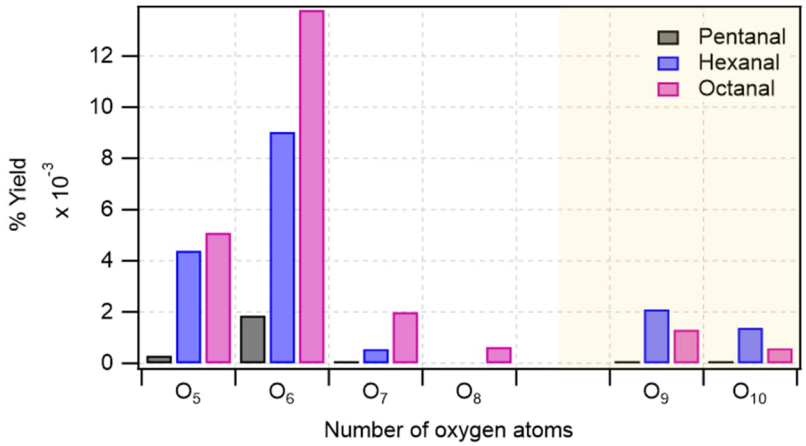

Figure 4. Distribution of major oxidation products (O_5–O_8 in monomeric regime with white background, and O_9–O_{10} in accretion product regime with light gold background) in pentanal, hexanal, and octanal oxidation initiated by OH radical. In y-axis, the numbers are the cumulative sum of yields of products with the same oxygen number. Reaction time, Δt = 11–13 s.

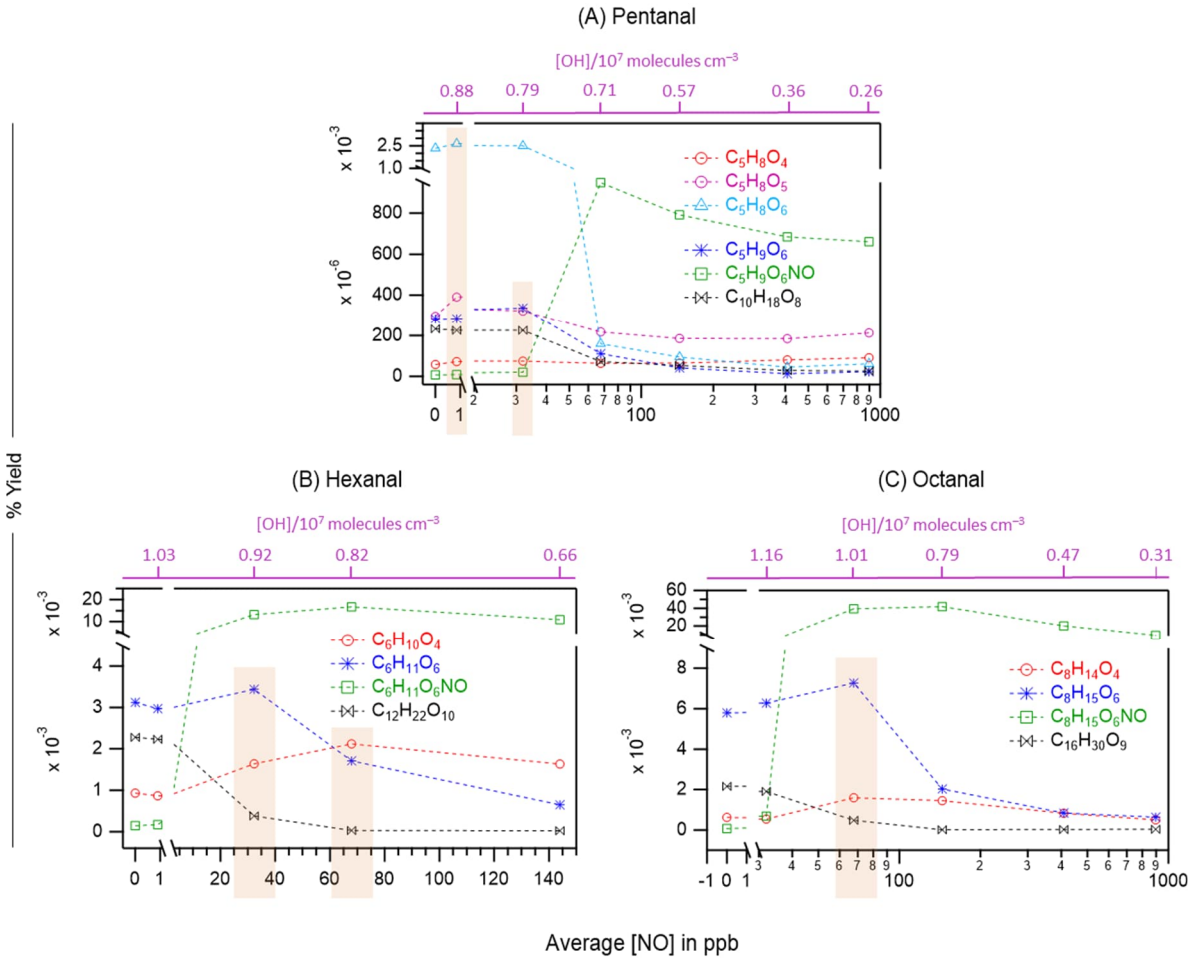

Figure 6. The yields of different oxidation products including monomeric HOMs, organonitrates (green markers), and HOM accretion products (black markers) as a function of average NO concentrations in OH initiated oxidation of n-aldehydes: pentanal (A), hexanal (B), and octanal (C). The corresponding average OH radical concentrations in these experiments are shown with purple scales. Note the logarithmic scale (x-axis) in panels A and C. The orange rectangles highlight the enhanced yields of several non-nitrogen containing products: O_4–O_6 closed-shell products from pentanal under around 1 ppb NO (A), O_4 closed-shell products from hexanal and octanal under around 70 ppb NO (B and C), O_6 peroxy radical from pentanal and hexanal under around 30 ppb NO (A and B) and the same from octanal under 70 ppb NO (C). Reaction time, Δt = 11–13 s.

2. The concentrations of precursor concentrations (a few ppm) appear to be much higher than ambient atmospheric conditions, which affects RO2 concentrations and fates. As the authors mentioned that some of key RO2 observed in this study were formed via bimolecular reactions, I suggest some discussion regarding the influence of RO2 concentrations on product distribution in this study and comparison of the RO2 fates with those in the ambient atmosphere, and how this would affect the formation of low volatility condensable materials.

Response: We thank the reviewer for the comment. In our flow reactor experiments, the oxidant OH radical was produced in situ by the ozonolysis reaction of TME (tetramethylethylene). We used high precursor VOC concentrations to scavenge OH, especially

as TME reacts so fast with it. On the other hand, the formation of initial RO_2 radicals, that drive subsequent autoxidation and HOM formation, in VOC + OH reaction in the flow reactor is limited by the concentration of reactant OH radicals (limiting reactant) despite having a higher VOC concentration.

We have now investigated the concentrations of initial RO_2 radicals formed in different *n*-aldehyde oxidation experiments using kinetic simulations and discussed them by adding a new section (*S13. Kinetic simulation*) in the Supplement. The whole section is reproduced here in pages 12–18 above.

3. L238-241, I suggest adding (Yan et al., 2020) and (Shen et al., 2022).

Response: We thank the reviewer for the suggestion. The citations (Yan et al., 2020) and (Shen et al., 2022) are now added to lines 273–274 in the revised manuscripts.

4. .L353-354, what is the " highest intensity" compared with?

Response: In the presence of high NO concentrations, HOM-ONs formed with the highest yields compared to neighboring non-nitrogen HOMs.

Changes to manuscript: In lines 390–392, "The experiments in the presence of high NO concentrations (30 ppb and above) produced the highest yields of HOM-ONs, compared to neighboring non-nitrogen HOMs, with the expense of HOM accretion products."

5. L352-353, can the authors specify what bimolecular reactions and what conditions are referred to as this statement clearly depend on reactions conditions such as RO2 and NO concentrations.

Response: We thank the reviewer for pointing out this. In the sentence in question, the possible bimolecular reaction partners are now specified.

Changes to manuscript: In lines 388–390, "... while the subsequent unimolecular rearrangements of the RO_2 intermediates are in competition with bimolecular reactions including other RO_2, HO_2, and NO_x."

References

Shen, H., Vereecken, L., Kang, S., Pullinen, I., Fuchs, H., Zhao, D., and Mentel, T. F.: Unexpected significance of a minor reaction pathway in daytime formation of biogenic highly oxygenated organic compounds, Science advances, 8, eabp8702, 10.1126/sciadv.abp8702, 2022.

Yan, C., Nie, W., Vogel, A. L., Dada, L., Lehtipalo, K., Stolzenburg, D., Wagner, R., Rissanen, M. P., Xiao, M., Ahonen, L., Fischer, L., Rose, C., Bianchi, F., Gordon, H., Simon, M., Heinritzi, M., Garmash, O., Roldin, P., Dias, A., Ye, P., Hofbauer, V., Amorim, A., Bauer, P. S., Bergen, A., Bernhammer, A. K., Breitenlechner, M., Brilke, S., Buchholz, A., Mazon, S. B., Canagaratna, M. R., Chen, X., Ding, A., Dommen, J., Draper, D. C., Duplissy, J., Frege, C., Heyn, C., Guida, R., Hakala, J., Heikkinen, L., Hoyle, C. R., Jokinen, T., Kangasluoma, J.,

Kirkby, J., Kontkanen, J., Kurten, A., Lawler, M. J., Mai, H., Mathot, S., Mauldin, R. L., Molteni, U., Nichman, L., Nieminen, T., Nowak, J., Ojdanic, A., Onnela, A., Pajunoja, A., Petaja, T., Piel, F., Quelever, L. L. J., Sarnela, N., Schallhart, S., Sengupta, K., Sipila, M., Tome, A., Trostl, J., Vaisanen, O., Wagner, A. C., Ylisirnio, A., Zha, Q., Baltensperger, U., Carslaw, K. S., Curtius, J., Flagan, R. C., Hansel, A., Riipinen, I., Smith, J. N., Virtanen, A., Winkler, P. M., Donahue, N. M., Kerminen, V. M., Kulmala, M., Ehn, M., and Worsnop, D. R.: Size-dependent influence of NO_x on the growth rates of organic aerosol particles, Science Advances, 6, 9, 10.1126/sciadv.aay4945, 2020.

Referee #4

The manuscript Barua et. al. reports the formation of HOMs due to oxidation of C5-C8 aldehydes, with their flow tube setup and subsequent analysis via mass spectrometry. Length of the aldehydic carbon chain directly affected the oxidation products. Molecules with longer carbon atoms produced HOMs with higher intensities. Addition of NO and its effect on HOM accretion products are discussed for different concentrations of NO.

General comments:

The experiments are well designed, results are clearly shown, and the manuscript is structured properly. The relevance of aldehydes and understanding their role in SOA formation is important for atmospheric chemistry research. The manuscript could be enhanced by adding some statistical insights perhaps (e.g. linear regression tests) on the observed trends, provided the dataset permits statistical analysis.

Response: We appreciate the reviewer's suggestion. The focus of the study is how efficiently HOMs can be formed in C_5–C_8 linear aldehydes that involve sequential oxidation processes. Due to the general complexity of the HOM formation process with contributions from multiple reaction pathways, it is not usual to have a linear relationship between HOM yields and number of carbon atoms of the precursor VOCs even if they belong to the same class (e.g., aldehydes). The same, i.e., non-linear effect of carbon chain length on HOM yields, is observed in this work (Figure 4). For the same reason, a linear trend on HOM yields with varying concentrations of the reactant VOC is not expected either (= we did not observe). Also, the observed non-linear trends from the experiments with varying NO concentrations (Figure 6) do not enable us to perform the regression tests.

Besides that, here are some 'Specific comments' for consideration:

L29: '…to the aerosol material that is formed by….'

Firstly, the term 'particle' could be used instead of 'material'.

Response: We thank the reviewer for the suggestion. However, we are referring to the SOA material that condenses on top of existing seed particles, and we do not expect these to form particles on their own. Therefore, we prefer using "material" which is a mixture of primary and secondary components, instead of using "particle" and apologize if this was unclear. Indeed, the subsequent sentences detail the process further. Additionally, we now stated the involvement of other processes also in the revised manuscript as shown in the reply to reviewer's next comment.

Secondly, from this sentence it seems oxidation of VOCs is the only method for SOA formation. In L39, the authors mention '...its sources and formation processes are yet to be fully understood.' It would be informative for the reader to know what other processes can lead to the formation of SOA. Not necessarily in detail but stating the other processes in the beginning might be useful for the reader.

Response: We thank the reviewer for pointing out this. Involvement of other processes is now included in the revised manuscript.

Changes to manuscript: In lines 29–31, "Secondary organic aerosol (SOA) refers to the aerosol material that is mainly formed by the atmospheric gas-phase oxidation of volatile organic compounds (VOCs) (Kroll and Seinfeld, 2008; Ziemann and Atkinson, 2012; Seinfeld and Pandis, 2016)."

Addition to manuscript: In lines 35–38, "However, heterogeneous and multiphase chemistry involving the reactions of organic compounds directly onto solid particles or inside liquid particles can also be an important contributor to SOA mass (Ervens et al., 2011, 2014; Kuang et al., 2020; Gu et al., 2023)."

L56-61: 'In high NOx (NO + NO2) condition…' Splitting this sentence would make the text easier to follow.

Response: We thank the reviewer for the suggestion. Accordingly, we made changes to the revised manuscript.

Changes to manuscript: In lines 59–65, "The aldehydic H abstraction can lead to the cleavage of that carbon (C1) by CO loss from acyl (RC(O)) intermediate (Rissanen et al., 2014; Barua et al., 2023). Alternatively, it leads to the acyl peroxy (RC(O)OO) and, in high NO_x ($NO + NO_2$) condition, subsequently to acyloxy (RC(O)O) intermediate followed by CO_2 loss ultimately forming C_{n-1} aldehyde, C_{n-1} alkyl nitrate, and C_{n-1} alkoxy isomerization products (Vereecken & Peeters, 2009; Chacon-Madrid et al., 2010)."

L62-65: 'Besides, it can also produce…' same as the previous comment. Splitting the sentence with their respective references is suggested.

Response: We thank the reviewer for the suggestion. Accordingly, we made changes to the revised manuscript.

Changes to manuscript: In lines 65–69, "Besides, it can also produce C_n peroxyacyl nitrates (PAN) via RC(O)OO + NO_2 reaction (Mellouki et al., 2003; Chacon-Madrid et al., 2010;

Calvert et al., 2011; Mellouki et al., 2015), a reservoir species for long-range transport of NO_x in the free troposphere. Additionally, C_n peroxy acids can be formed by the reaction of RC(O)OO intermediate and HO_2 (Barua et al., 2023)."

L89: ' …competitive for autoxidation reaction chain propagation…' this phrase seems too long winded. Some alternative suggestions for rephrasing: "…competitive with chain propagation in autoxidation…" or "…competitive with autoxidation chain-propagation reactions…". Either usage depends on which aspect of the phrase the authors want to emphasize on.

Response: We thank the reviewer for the suggestion. The sentence in question is now rephrased and split into two for better clarity in the revised manuscript.

Changes to manuscript: In lines 90–94, "Along the aldehydic H abstraction reaction route, the fastest isomerization (1,6 H-shift rate coefficient, $k = 0.2\ s^{-1}$) of the RC(O)OO intermediate was shown to be the key for autoxidation reaction chain propagation and competitive with any bimolecular reaction mediated RC(O)O fragmentation (Barua et al., 2023). Thus, the RC(O)OO isomerization reaction (Seal et al., 2023) keeps the carbon backbone of the precursor aldehyde intact."

L109: 'Fig. S1 in the Supplement…' It might be convenient for a reader who is not directly related to such experiments, to have the experimental schematic or a flowchart appear in the main manuscript, rather than in a supplement.

Response: We thank the reviewer for the suggestion. Figure S1 was previously used in our hexanal paper (Barua et al., 2023) which is why it was provided in the Supplement of this work. To avoid self-plagiarism, we now produced another schematic of the experimental setup and added it to the main manuscript (Figure 1 below).

Addition to manuscript:

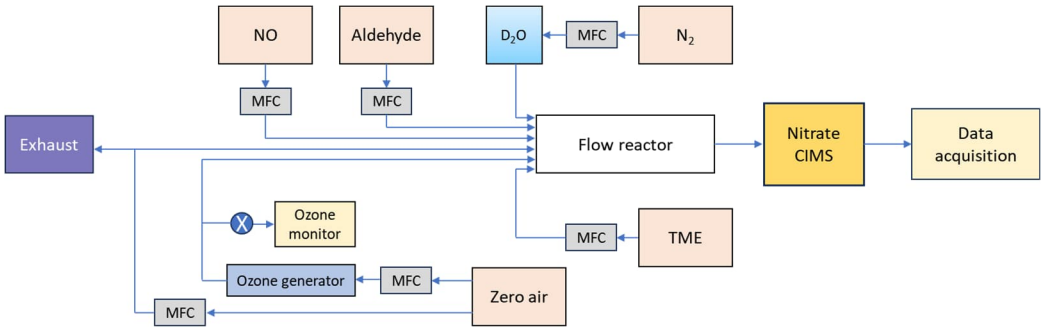

Figure 1. Schematic representation of a flow reactor setup showing a nitrate (NO_3^-) based chemical ionization mass spectrometer coupled to ambient pressure flow reactor. TME = tetramethylethylene (C_6H_{12}). The oxidant OH radical was produced in situ by TME + O_3 reaction. MFC = mass flow controller.

L139: omit 'also'

Response: We thank the reviewer for the suggestion. The word "also" is now removed from line 151 in the revised manuscript.

Some information on the data processing steps, e.g. baseline corrections, would be helpful for reproducibility. They could be added at the end of the Method section, where data analysis is mentioned.

Response: We thank the reviewer for the suggestion. We have now mentioned the data processing steps in the revised manuscript.

Changes to manuscript: In lines 164–166, "The mass spectrometric data processing, including averaging, baseline removal, mass axis calibration, and peak integration were done using the tofTools v6.03 package for MATLAB."

L180: comma after H-shift.

Response: We thank the reviewer for the suggestion. A comma is now put after "H-shift" in line 207 in the revised manuscript.

L181-184: Splitting the sentence is suggested after 'while'.

Response: We thank the reviewer for the suggestion. The sentence is now split into two in the revised manuscript.

Changes to manuscript: In lines 208–213, "As the reaction time increased, we observed the formation of monomeric HOM up to O_7 and accretion products up to O_{10} composition within 2.9 s in hexanal oxidation (see Fig. 2D) with the consumption of $\sim 8.88 \times 10^{-4}$ of its initial concentration. In the case of octanal, monomeric O_8 HOM and accretion products up to O_{10} formed within 2.1 s reaction time (see Fig. 2E) with a comparable reacted fraction ($\sim 8.71 \times 10^{-4}$) of its initial concentration."

L200: Typo 'withing'

Response: We thank the reviewer for pointing out this. The spelling is now corrected (i.e., "within") in line 230 in the revised manuscript.

L205-206: '….while heptanal produced most oxygenated products are C7H12–14O8 (see Figure 2C)'. Grammatically incorrect. Kindly rephrase.

Response: We thank the reviewer for the suggestion. The sentence in question is now rephrased in the revised manuscript.

Changes to manuscript: In lines 234–236, "Figure 3D implies that the highest oxygenation ($C_8H_{15}O_9$) in the monomeric HOM products is associated with octanal, whereas Fig. 3C shows that the most oxygenated products produced from heptanal are $C_7H_{12-14}O_8$."

L307: References should be in ascending chronological order. Also, in L42, L 64, L330, etc., and many other instances, the reference order is mixed up. Kindly check throughout.

Response: We thank the reviewer for pointing out this. The reference order is corrected in the revised manuscript.

L356: '…various NO conditions'. Could the conditions be specified here briefly, for which conditions the oxidation products were enhanced.

Response: We thank the reviewer for the suggestion. In the sentence in question, the NO conditions that showed enhancement effects with the oxidation products are now specified in the revised manuscript.

Changes to manuscript: In lines 392–394, "However, some enhancements with the yields of low oxygenated closed-shell products and O_6 peroxy radicals were also seen under 1–70 ppb NO conditions."